13th International Conference on Wind Engineering, Amsterdam, The Netherlands,
July 10-15, 2011

Commentary on the Indian Standard for Wind Loads

K. Suresh Kumar

RWDI India, T5 Thejaswini, Technopark, Trivandrum, Kerala, India, suresh.kumar@rwdi.com

ABSTRACT

This paper elaborates on how well the Indian Standard for wind loads (IS:875) predicts the wind-induced local loads as well as overall structural loads on tall buildings in conjunction with reality. For this investigation, the wind tunnel results from a standard CAARC building model have been utilized for comparing against the IS:875 predictions. Further, predictions from other international codes of practice and from few Indian projects are also included in this paper for comparison purposes. Based on this study, preliminary recommendations have been made.

KEY WORDS: CAARC, Indian Standard, IS:875, Wind loads, Wind tunnel.

1 INTRODUCTION

The Indian standard of practice (IS:875 Part 3, 1987) is widely used for estimating wind loads by practitioners in India. Prem Krishna (2006) and Subhash and Tamura (2007) discussed the need for an immediate review of the IS:875 and recommended further investigations. Based on our comparison of tunnel results with the codes, the IS:875 to our surprise stood apart from other codes and quite differently from the wind tunnel results. This led us to embark on a test project to compare the IS:875 predictions with the wind tunnel results for a standard building. The widely tested CAARC building model (Melbourne, 1980) has been chosen for this study. Considering that the standards are based on simple box-like structures without any immediate surroundings, it is expected the wind tunnel results of CAARC model in line with values from codes of practice. This paper presents both cladding and structural load comparisons between wind tunnel tests and IS:875 including the predictions from other international standards. Note that only vertical facades have been considered for the local wind loads considering the significant usage of glazing.

2 EXPERIMENTAL SETUP

The data presented here were collected from wind tunnel studies of the standard CAARC tall building model using the HFPI (High Frequency Pressure Integration) technique. The HFPI method is based on the simultaneous measurement of pressures at several locations on a building. The CAARC is a simple rectangular box type building without any architectural features/geometric disturbances such as parapets, balconies, fins, mullions etc. These tests were conducted on a 1:400 scale model of the building without immediate surroundings, as shown in Figure 1, in RWDI's 2.4m x 2.0m boundary-layer wind tunnel. A rural upwind terrain condition (z_o = 0.1m, corresponding approximately to a power law exponent of 0.17) was simulated for all wind directions by means of floor roughness and upwind spires.

For the HFPI tests, the building was instrumented with 280 pressure taps, including the standard CAARC locations, plus additional taps near the building edges. Time series of the pressures at these locations were collected and stored for post-test analysis. The individual pressure time series were used to form time series of the base loads and generalized forces, from which statistics and spectra were calculated. Thereafter, the peak base moments, shears and torsion were determined. Also, this data were used to derive the local pressure statistics.

Figure 1 provides the pressure tap locations for the HFPI study, along with the overall equivalent full-scale dimensions (height = 182.88m), axes system and wind flow angle. The wind tunnel tests were conducted for 36 wind directions at 10^o intervals.

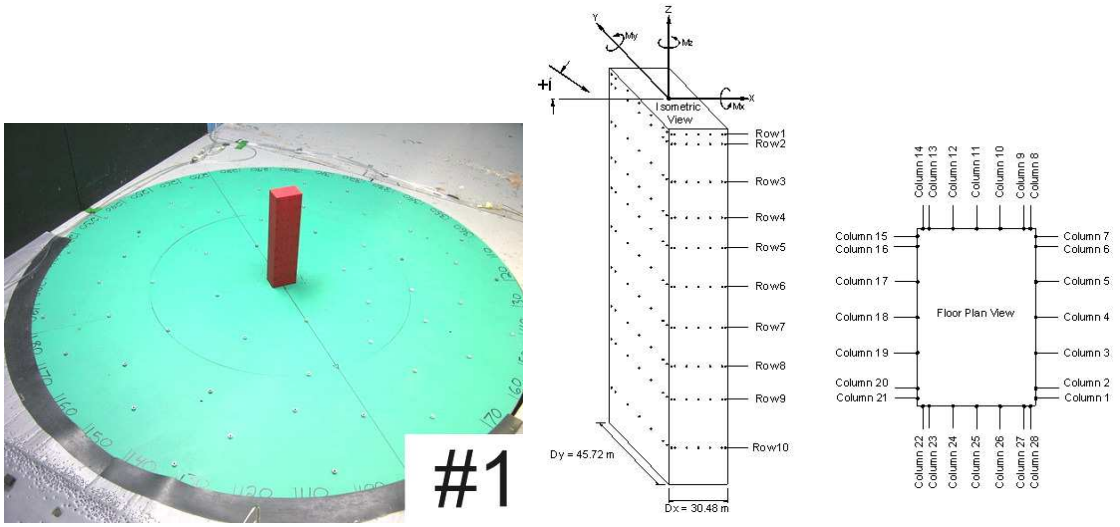

Figure 1. CAARC building model in wind tunnel - pressure tap locations.

For the analysis, the full scale natural frequency of the building was taken as 0.2 Hz in both sway directions and 0.3 Hz in the torsional direction. The structural damping was taken as 1% of critical and the mass distribution of the building was taken to be 160 kg/m^3. These above values were the same as used in the previous CAARC studies (Dragoiescu et al., 2006; Melbourne, 1980).

The mean, root-mean-square, peak maximum and peak minimum values of the pressure signals were measured for all wind directions. Note that peak local pressure values correspond to an averaging time of about 1-sec. All pressure measurements were carried out with a free stream wind velocity of approximately 15m/s.

3 LOCAL WIND LOADS

Local mean and rms pressure coefficients corresponding to the ring of taps from row 4 located approximately at 2/3rd height (see Figure 1) are shown in Figure 2 for a wind direction of 0°.

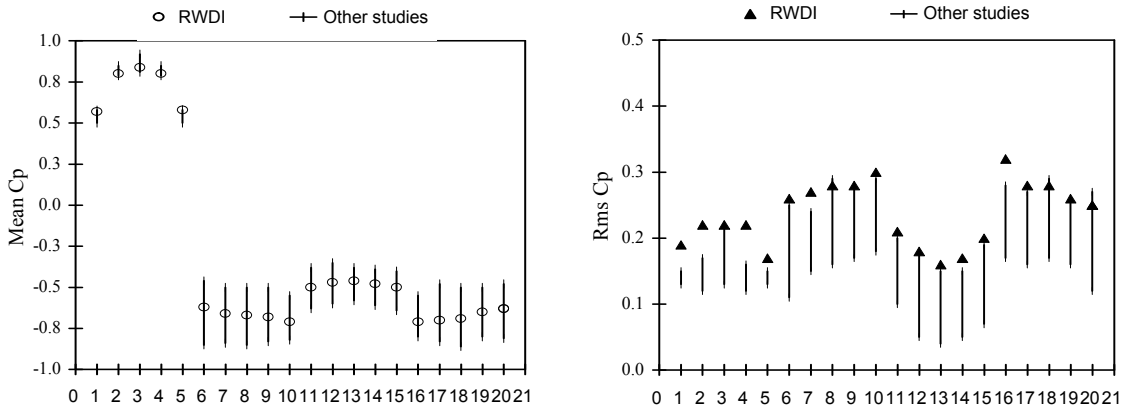

Figure 2. Comparison of pressure coefficients – RWDI vs Other studies.

Also in this figure, range of results from previous studies at 2/3rd height for a wind angle of 0° is also presented for comparison. Note that the present study had eight extra taps at the corners in each row and these taps have been avoided in this comparison to be similar with other studies. The results show a good degree of agreement and the observed deviations are mainly due to distortion of length scale, wind tunnel blockage effect and profile variations.

To get an insight into the wind tunnel results, peak factors and gust factors are derived and plotted in Figure 3. Peak factors (gp neg & gp pos) are defined as (peak-mean)/rms, while gust factors (G neg & G pos) are defined as peak/mean. As expected, the negative peak factors are much higher than positive peak factors. Considering the flow separation at edges and high negative pressures, the negative peak factors are getting as high as 12, while the mean of the positive peak factors are about 5 only. On the same token, the negative gust factors are also getting much higher than positive gust factors. Note that the positive gust factors are clustered around 3 which is closer to the 2.5 value used in NBC code.

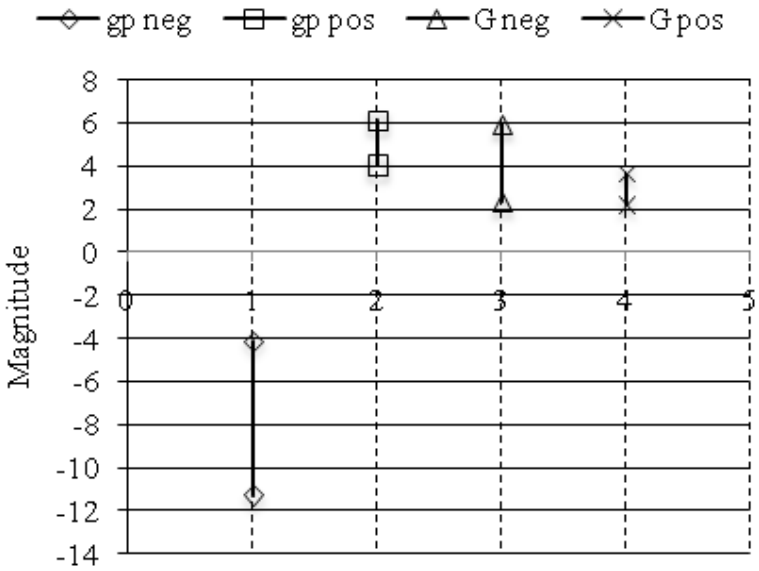

Figure 3. Peak factor and Gust factor.

To bring the wind tunnel results in similar format with the IS and ASCE codes, the wind tunnel results have been converted to pressure coefficients based on peak dynamic pressure at roof height. These results have been plotted in Figure 4 for selected elevations at corresponding tap locations for negative and positive pressures. The provided pressure coefficients in Figure 4 are minimum and maximum pressure coefficients at individual tap locations irrespective of the angle of attack.

Negative pressure coefficients are higher at the edges and moderate at the center as expected from typical flow regime. However, in case of positive pressure coefficients, they seem to increase along the height with the exception of extreme top region where they reduce as the flow tries to escape. Along with the wind tunnel results, the pressure coefficients from ASCE7-05 (2005), NBC2005 (2005) and IS:875 are also provided at the top. Note that equivalent NBC pressure coefficients in the same format as those with ASCE and IS have been derived and presented in this plot.

As far as the negative pressure coefficients are concerned, IS:875 value is -1.2 and this code does not distinguish between edge and center zones. This coefficient is much lower than the edge zone pressure coefficients obtained from wind tunnel results. Also, ASCE and NBC codes provide higher values as well for edge zones. However, IS and NBC values for center zone seem

closer to the wind tunnel predictions. Note that certain variations in pressure coefficients can be attributed to the conversions from one format to the other. Overall, we can infer that the IS:875 significantly underestimate loads on claddings located especially on the edges. Also it appears that some of the local pressure coefficient data on the standard could have been obtained under smooth flow conditions and this may be the reason for a lower value. As far as the positive pressure coefficients are concerned, the wind tunnel results are in good match with ASCE and NBC values, while the IS:875 is not providing any value.

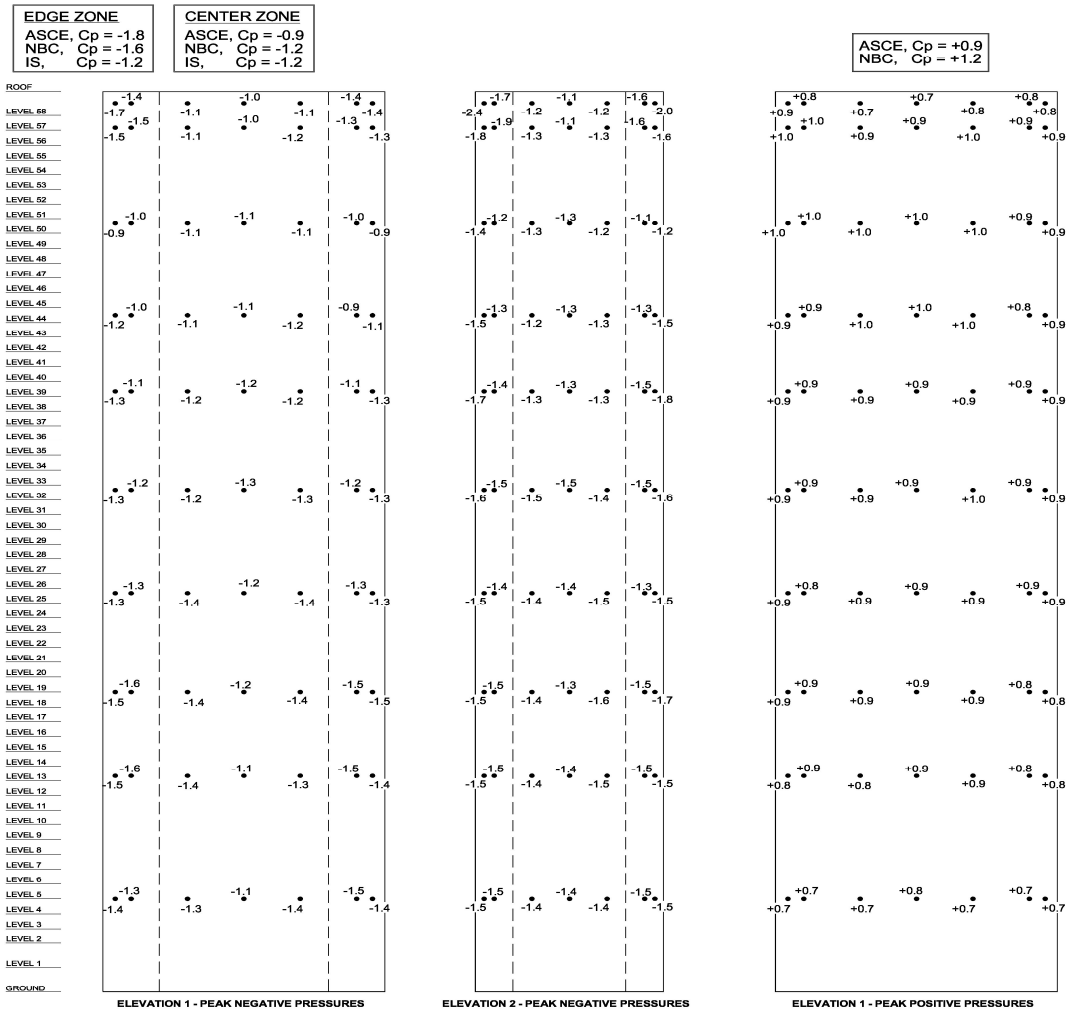

Figure 4. Peak pressure coefficients on CAARC facades.

Finally, an example has been worked out for predicting local cladding load on a CAARC type building in Mumbai using wind tunnel and various codes. The basic wind velocity for Mumbai of 44 m/s 3-sec gust has been used for this exercise. Figure 5 shows the comparison of peak negative pressures along the height of the building. Note that the wind tunnel predicted cladding loads are between ASCE and NBC predictions, while the IS code predictions are far below. When the average wind tunnel predicted pressure is -3.75 kPa, the maximum IS prediction is only -2.3 kPa. This result shows that the IS code under-predicts cladding loads significantly and the code should be used with caution. Similarly, the positive pressure distributions have been compared in Figure 5. Note that the wind tunnel predictions are between the ASCE and NBC codes. However, the IS code does not provide any positive pressure value.

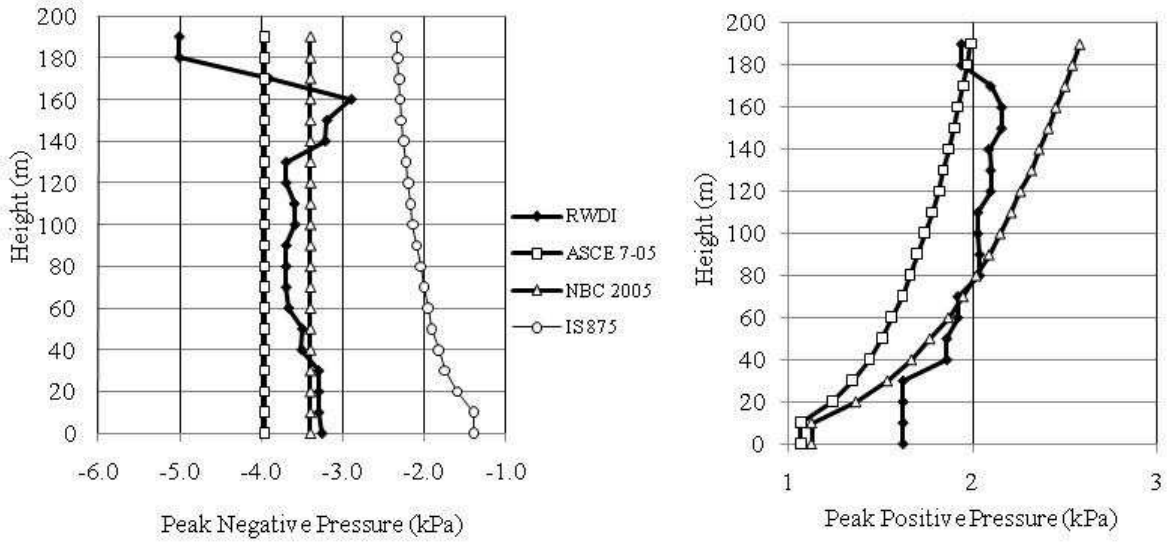

Figure 5. Comparison of peak pressures on CAARC building.

In a recent three tower project (heights of the order of 350m) in Mumbai, the IS:875 prediction of the external pressure was -2.5kPa, while ASCE7-05 predictions were -2.5kPa & -4.5kPa. The wind tunnel predictions went up to -6kPa though these high values were hot-spots at isolated locations on the façade. The more typical wind tunnel values on majority of the façade were within the ASCE predictions, but much higher than the IS:875 value.

4 OVERALL WIND LOADS

The mean base overturning moments normalized with $\frac{1}{2}\rho U_H^2 H^2 D_y$ are shown in Figure 6, where U_H = reference velocity at roof height, H = height (182.88 m) and D_y = wide dimension of building cross section (45.72 m). The plots also show the corresponding range of results from other studies (Melbourne, 1980). Equivalent mean base overturning moment coefficients for orthogonal directions were also derived and plotted in Figure 6 corresponding to IS and ASCE

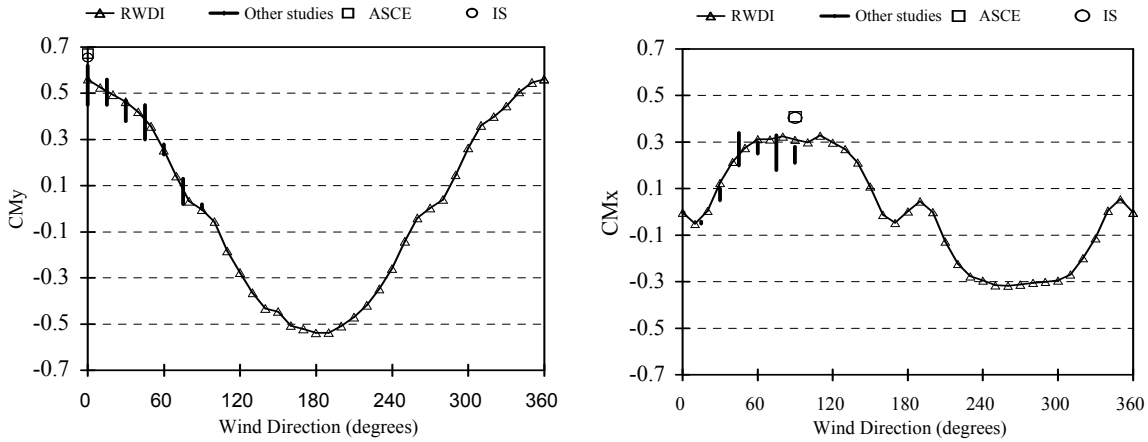

Figure 6. Wind-induced mean response of CAARC building.

codes. The results from RWDI and the codes on the standard CAARC model compare reasonably well with results predicted by others in the past. Part of the variation would be the result of differences in the flow simulations. The previous studies were conducted in rougher terrain (suburban or rougher) simulations compared to the rural type terrain condition used for this study.

For the analysis, full-scale 3-sec gust wind speed of 44 m/s at 10 m height in open terrain is used. The raw overall base moments (maximum, mean and minimum) obtained from the tunnel for each wind direction are plotted in Figure 7. It can be noticed that there is across-wind loading at angles 90° and 270° in the X direction (see My), while the across-wind loading is dominating in the Y direction for wind angles 0° and 180° (see Mx). Considering the aspect ratio, as expected the across-wind effects are significant along the Y-dir when the wind is blowing perpendicular to the wider face or along X-dir. Winds blowing along Y-dir also induce across-wind loading in the X-dir but only as high as the along-wind loading. Note that mean loading will peak at the along-wind loading condition in comparison to the zero or minimum mean value at the across-wind loading condition due to the symmetry of the flow.

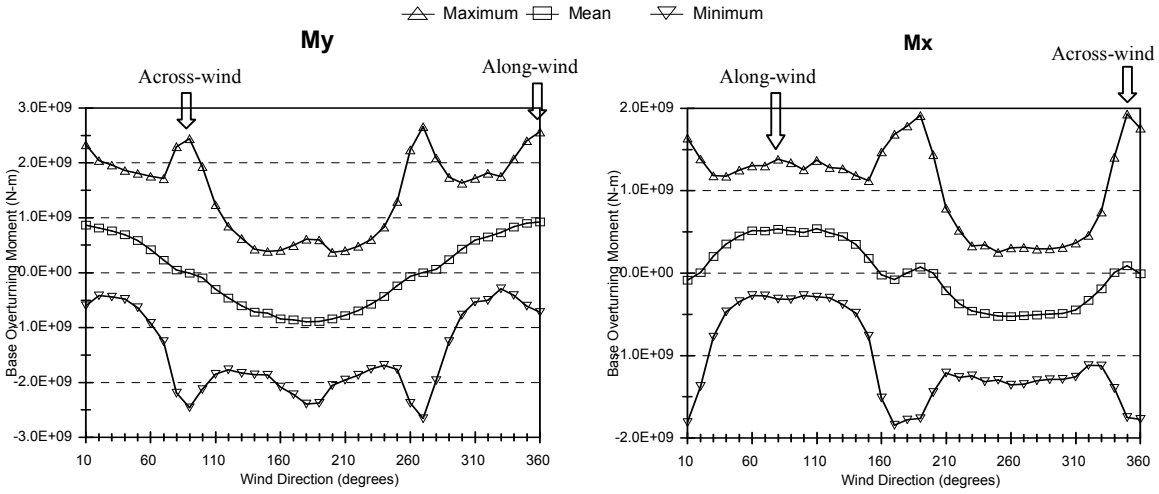

Figure 7. Raw overall base moments on CAARC building.

The overall peak base loads calculated analytically using the IS:875 is compared against ASCE and the wind tunnel values, and they are presented in Table 1. The results show that the values predicted in the X direction using IS:875 are generally in good agreement with the tunnel values, while the ASCE values are lower. In the Y-direction, both IS and ASCE are predicting lower values than the tunnel values. It is observed from Figure 7 that the peak along-wind loading compares well with the code predicted values for both directions. This shows that the tunnel predicted peak values are based on across-wind loading when both codes are predicting along-wind loads. In summary, the codes will under predict the loads in cases where across-wind phenomenon is dominating.

Table 1. Overall base loads on CAARC building.

	Fx (kN)	Fy (kN)	My (kN-m)	Mx (kN-m)	Mz (kN-m)
IS	2.39E+04	1.54E+04	2.42E+06	1.56E+06	-
ASCE	2.27E+04	1.41E+04	2.18E+06	1.36E+06	1.57E+05
RWDI	2.39E+04	1.64E+04	2.66E+06	1.93E+06	1.55E+05

At all angles of attack, buildings will be subjected to simultaneous action of sway loading at orthogonal directions as well as torsional loading. But the torsional loading didn't get the needed attention in many international codes of practice similar to IS code. In case of taller/slender buildings with lack of torsional stiffness caused by inefficient structural systems, torsional response/loading becomes even more important in comparison to the short/stiff building. Figure 8 shows the torsional loading measured on the CAARC building. Note that sharp flow separations at skewed angles (90^o & 270^o) of flow against the narrow face induce peak torsional forces on the building. In a square building scenario, peak torsional loading of equal magnitude will occur at four locations at skewed angles of flow against the four faces. In this case, the peak torsional moment is normalized by the maximum shear force as well as width to get the torsional eccentricity factor (e). The torsional eccentricity factor (e) for this case is about 15%. Based on numerous such studies in our lab and elsewhere, the torsional eccentricity factor typically ranges between 5% and 25% depending on the geometry and the surroundings. For preliminary estimation purposes, a torsional eccentricity factor (e) of 15% can be used similar to ASCE code. The torsional moment (Mz) at floor levels can be calculated by multiplying the maximum shear (F) with maximum width (B) and 15% torsional eccentricity factor; i.e. Mz = F x B x 0.15.

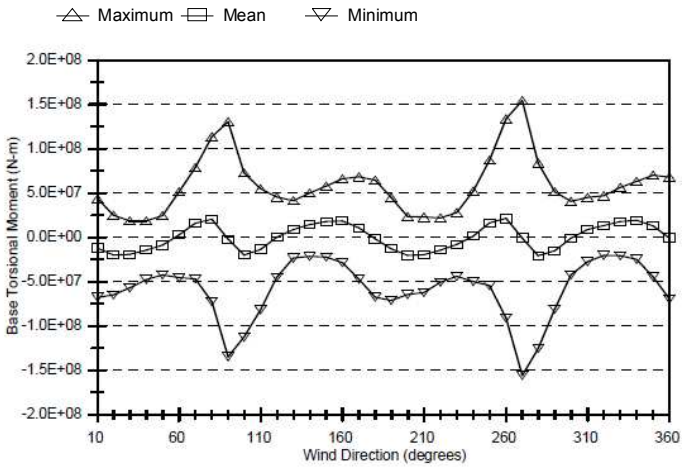

Figure 8. Overall torsional moment on CAARC building.

In a recent tall building project (height~250m) in Mumbai, wind-induced loading on orthogonal directions were higher than the IS code predictions (see Table 2). Significant difference in the Y-direction load was due to across-wind phenomenon caused by peculiar geometry.

Table 2. Overall base loads on a tall building project in Mumbai.

	Fx (kN)	Fy (kN)	My (kN-m)	Mx (kN-m)
IS	2.43E+07	3.81E+07	3.59E+09	5.40E+09
RWDI	3.34E+07	9.75E+07	5.46E+09	1.69E+10

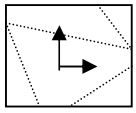
PLAN

In another project in Mumbai, structural engineers didn't give any consideration for simultaneous action of sway forces in orthogonal directions and torsional forces in their preliminary design based on IS:875. For this particular project, the wind tunnel results were lower than the individual code derived forces and as a result the team was happy initially before they realized about the simultaneous action of the three forces and the associated load combinations. Once the simultaneous action of the loads is accounted, then the resultant forces were higher than the individual code derived forces. We have noticed that this is particularly happened since there is no recommendation or not even a wording on this issue anywhere in IS:875. Considering the importance of this matter, at least provisions made in other international codes (ASCE7-05, 2005; NBC2005, 2005) should be considered at the earliest.

5 RECOMMENDATIONS

Based on this study, the following recommendations have been made for practitioners while using the IS:875 code for wind load calculations.

It is recommend the local pressure coefficient to be increased to -1.8 from the current value of -1.2 at least for an edge zone of 20% building width. For the central region, one can use the same pressure coefficient of -1.2 currently in the code. The practitioners can use the load calculation procedure in IS:875 with minimum risk (r=0.63, life of 50 years) by using the above recommended pressure coefficients.

Cross-wind effects should be assessed using other international codes of practice until such procedure shows up in the next revision of IS. Torsional loading shall be calculated based on maximum shear force, maximum width and a torsional eccentricity factor of 15% (Mz = F x B x 0.15). Based on our wide experience in the subject matter, for simultaneous application of loads, 100% of any individual primary force (Fx, Fy or Mz) can be considered with 60% of secondary forces (Fx, Fy or Mz).

6 CONCLUDING REMARKS

The results of this study indicate that concerning the cladding loads predicted by IS:875, the pressure values on edges stand much lower than the tunnel tested and ASCE values. Therefore, IS:875 predictions for cladding design should be used with caution and it is strongly recommended to look at other international codes at the preliminary design stage. Also, it is necessary to revamp the tabular values for external pressure coefficients provided for local cladding design at the earliest.

The structural load comparisons indicate that IS:875 is indeed good enough for preliminary structural load predictions in the absence of across-wind response domination. However, the necessity of including a basic estimation procedure for across-wind response is clear which will help practitioners accounting this phenomenon in early stage of the design itself. Provision for torsional loading should also be included in the code. Further, simultaneous application of sway forces and torsional loads with suggested combination factors shall be included as well.

This paper mainly addressed the local wind loads on vertical facades as well as overall structural loads on tall buildings. Many other subject matter from the IS:875 standard such as wind speed map, loading on roof and other structures requires revision as well. There are number of typographical errors in various tables and figures and the user needs to review the selected values thoroughly before using it in the current format. In summary, it is vital that the review and update of the existing provision (IS:875 Part 3, 1987) shall be carried out at the earliest.

7 REFERENCES

ASCE7-05, 2005. Minimum Design Loads for Buildings and Other Structures. Structural Engineering Institute of ASCE, Reston, VA.

Dragoiescu, C., Garber, J., Suresh Kumar, K., 2006. A Comparison of force balance and pressure integration techniques for predicting wind-induced responses of tall buildings, in: Proceedings of the ASCE Structures Congress 2006 – Extreme Wind Engineering, St.Louis, USA.

IS:875 Part 3, 1987. Code of Practice for Design Loads (Other than Earthquake) For Buildings and Structures, Part 3 Wind Loads. Bureau of Indian Standards, New Delhi.

Melbourne, W.H., 1980. Comparison of measurements on the CAARC standard tall building model in simulated model wind flows. Journal of Wind Engineering and Industrial Aerodynamics 6, 73-88.

NBC2005, 2005. User's Guide NBC – 2005, Structural Commentaries (Part 4). Canadian Commission on Building and Fire Codes, National Research Council of Canada.

Prem Krishna, 2006. The Indian wind loading standard: A case for review, in: Proceedings of the 3rd National Conference on Wind Engineering, 35-34, Kolkata, India.

Subhash, C.Y., Tamura, Y., 2007. Some issues concerning to the Indian wind loading standard [IS:875 (Part 3) – 1987], in: Proceedings of the 12th International Conference on wind Engineering, 2679-2686, Cairns, Australia.